tion alters the thermal structure of the deep ocean (25). Calculations for such extended periods are beyond the scope of this study.

REFERENCES AND NOTES

1. Climate: Long-Range Investigation, Mapping, and Prediction (CLIMAP) Project Members, *Map and Chart Series MC-36* (Geological Society of America, Boulder, CO, 1981).
2. T. P. Guilderson, R. G. Fairbanks, J. L. Rubenstone, *Science* **263**, 663 (1994).
3. M. Stute *et al.*, *ibid.* **269**, 379 (1995).
4. D. Rind and D. Peteet, *Quat. Res.* **24**, 1 (1985).
5. L. G. Thompson *et al.*, *Science* **269**, 46 (1995).
6. W. S. Broecker, *Quat. Res.* **26**, 121 (1986); M. W. Lyle, F. G. Prahl, M. A. Sparrow, *Nature* **355**, 812 (1992).
7. J. E. Kutzbach and P. J. Guetter, *J. Atmos. Sci.* **43**, 1726 (1986).
8. N. M. J. Hall, P. J. Valdes, B. Dong, *J. Clim.* **9**, 1004 (1996).
9. S. Manabe and A. J. Broccoli, *J. Geophys. Res.* **90**, 2167 (1985).
10. A. J. Broccoli and S. Manabe, *Clim. Dyn.* **1**, 87 (1987).
11. S. G. H. Philander, *El Niño, La Niña, and the Southern Oscillation*, vol. 46 of *International Geophysics Series* (Academic Press, New York, 1990); J. D. Neelin, M. Latif, F.-F. Jin, *Annu. Rev. Fluid Mech.* **26**, 617 (1994).
12. D. Andreasen and C. Ravelo, *Paleoceanography* **12**, 395 (1997).
13. T. F. Pederson, *Geology* **11**, 16 (1983).
14. See a summary by T. J. Crowley and G. R. North [*Paleoclimatology* (*Oxford Monograph on Geology and Geophysics 18*, Oxford Univ. Press, New York, 1991)], pp. 56–57.
15. The horizontal redistribution of warm surface waters during El Niño alters the topography of the thermocline—it deepens in some regions and shoals in others—while leaving unchanged the spatially averaged depth of and the temperature difference across the thermocline. That is why two-layer models of the ocean are effective tools for studying El Niño.
16. Z. Liu and S. G. H. Philander, *J. Phys. Oceanogr.* **25**, 449 (1995); D. Gu and S. G. H. Philander, *Science* **275**, 805 (1997).
17. C. T. Gordon and W. Stern, *Mon. Weather Rev.* **110**, 625 (1982); R. C. Pacanowski, K. Dixon, A. Rosati, "The GFDL Modular Ocean Model user guide," *GFDL Ocean Group Tech. Rep. 2* (Geophysical Fluid Dynamics Laboratory, Princeton, NJ, 1991).
18. W. R. Peltier, *Science* **265**, 195 (1994).
19. R. G. Fairbanks, *Nature* **342**, 637 (1989).
20. S. Levitus, *NOAA Prof. Pap. 13* (U.S. Government Printing Office, Washington, DC, 1982).
21. S. G. H. Philander *et al.*, *J. Clim.* **9**, 2958 (1996).
22. A. E. Gill, *Q. J. R. Meteorol. Soc.* **106**, 447 (1980).
23. A. B. G. Bush and W. R. Peltier, *J. Atmos. Sci.* **51**, 1581 (1994).
24. W. T. Hyde, T. J. Crowley, K.-Y. Kim, G. R. North, *J. Clim.* **2**, 864 (1989).
25. D. P. Schrag, G. Hampt, D. W. Murray, *Science* **272**, 1930 (1996).

26. This work was supported by a Natural Sciences and Engineering Research Council of Canada grant OGP0194151 (A.B.G.B.) and by the National Oceanic and Atmospheric Administration under contract NOAA-NA56GP0226 (S.G.H.P.). We thank the staff of the Geophysical Fluid Dynamics Laboratory for making this work possible.

7 November 1997; accepted 20 January 1998

Molecular Mimicry by Herpes Simplex Virus–Type 1: Autoimmune Disease After Viral Infection

Zi-Shan Zhao, Francesca Granucci, Lily Yeh, Priscilla A. Schaffer,* Harvey Cantor

Viral infection is sometimes associated with the initiation or exacerbation of autoimmune disease, although the underlying mechanisms remain unclear. One proposed mechanism is that viral determinants that mimic host antigens trigger self-reactive T cell clones to destroy host tissue. An epitope expressed by a coat protein of herpes simplex virus–type 1 (HSV-1) KOS strain has now been shown to be recognized by autoreactive T cells that target corneal antigens in a murine model of autoimmune herpes stromal keratitis. Mutant HSV-1 viruses that lacked this epitope did not induce autoimmune disease. Thus, expression of molecular mimics can influence the development of autoimmune disease after viral infection.

Autoimmune diseases result from a loss of self-tolerance and the consequent immune destruction of host tissues (*1*). Although the pathology of the associated tissue destruction has been well characterized, the mechanisms responsible for initiation and pathogenesis of autoimmune diseases remain unclear. Several mechanisms have been proposed on the basis of the clinical observation that viral infections can induce or exacerbate autoimmune disease (*2*). Virus-induced inflammatory responses that result in release of self antigens and enhancement of costimulatory activity may trigger autoreactive T cells (*3*, *4*). It also has been proposed that viral determinants that mimic host antigens directly stimulate self-reactive T cell clones to attack sequestered host tissues (*5*). Certain viral peptides that cross-react with self peptides can stimulate autoreactive T cells (*6*), and mice genetically engineered to express a viral protein can develop autoimmune disease after infection with the relevant virus (*7*). However, these observations do not provide direct evidence that viral infection can precipitate autoimmune disease by mechanisms that include molecular mimicry. Herpes stromal keratitis (HSK), a disorder induced by HSV-1 infection and characterized by T cell–dependent destruction of corneal tissue, is a leading cause of human blindness (*4*, *8*). To examine the role of viral mimicry in autoimmune disease, we have now studied a murine model of HSK in which corneal HSV-1 infection reproducibly results in a T cell–mediated autoimmune reaction (*8*, *9*).

Murine HSK elicited by HSV-1 (KOS strain) in C.AL-20 mice is mediated by $CD4^+$ T cell clones specific for corneal self antigens but that also recognize a peptide (amino acids 292 to 308) in the C_H3 region of immunoglobulin $G2a^b$ ($IgG2a^b$) (*9*). However, the role of this virus in the induction of HSK disease was not investigated. Given that there are insufficient numbers of T cells in the cornea after HSV-1 (KOS) infection to define potentially cross-reactive cells (*10*), we investigated whether the HSK-inducing C1-6 and C1-15 T cell clones might also recognize HSV-1 epitopes by measuring their proliferative response after stimulation with HSV-1 antigens. Both HSK-inducing clones, but not the ovalbumin (OVA)-reactive clone O3 (*11*), were activated by extracts of HSV-1 (KOS)–infected Vero cells [10^5 ultraviolet (UV)-inactivated plaque-forming units (PFU) per milliliter] but not by extracts of uninfected Vero cells (Fig. 1A).

We searched the GenBank database for HSV-1 proteins that share sequence homology with the keratogenic peptide recognized by C1-6 and C1-15. The best match was with a peptide sequence embedded in the HSV virion-associated protein UL6 (*12*), which contains identical or similar amino acids at seven of eight sequential positions that contribute to T cell recognition (Arg-Lys-Ser-Asp-*Ser*-Glu-Arg-Gly; mismatched residue in italics) (*9*). Both keratogenic clones, but not the OVA-reactive clone, were activated by a synthetic 15-residue viral peptide based on UL6 (amino acids 299 to 314) [UL6-(299–314)] and containing this nested sequence, whereas an unrelated peptide derived from murine mammary tumor virus (MMTV) did not activate these two clones at any concentration tested (Fig. 1B).

The proliferative response of the two keratogenic $CD4^+$ T cell clones to the UL6-(299–314) peptide suggested that in-

Z.-S. Zhao, F. Granucci, H. Cantor, Department of Pathology, Harvard Medical School, and Department of Cancer Immunology and AIDS, Dana-Farber Cancer Institute, Boston, MA 02115, USA.
L. Yeh and P. A. Schaffer, Division of Molecular Genetics, Dana-Farber Cancer Institute, Boston, MA 02115 USA.

*Present address: Department of Microbiology, University of Pennsylvania School of Medicine, Philadelphia, PA 19104 USA.

travenous administration of the soluble peptide into susceptible C.AL-20 mice might inhibit development of HSK. Mice injected twice intravenously with soluble UL6 peptide before corneal inoculation of HSV-1 (5×10^4 PFU per cornea) did not develop HSK; in contrast, mice treated the same way with a control peptide from MMTV developed HSK (Fig. 2A). Immunization of mice with the UL6 peptide in adjuvant also might be expected to result in expansion of T cells capable of inducing HSK. Because immunization of mice with components of HSV-1 can inhibit the HSK response as a result of production of neutralizing antibodies to HSV-1 (*13*), we measured the ability of T cells from peptide-immunized C.AL-20 mice to induce HSK in adoptive syngeneic hosts that lack T cells. T cell–deficient BALB/c *nu/nu* (nude) mice that received T cells (5×10^6) from C.AL-20 mice immunized with UL6-(299–314) peptide in adjuvant developed severe HSK, but *nu/nu* recipients of the same number of T cells from C.AL-20 mice immunized with the MMTV control peptide did not develop significant disease (Fig. 2B).

To further define the role of the UL6-derived peptide in HSK, an HSV-1 (strain KOS) virus containing a mutation in the UL6 gene was produced (*14*). A single base pair substitution introduced by site-directed mutagenesis generated a stop codon in the 5′ end of the UL6 open reading frame (Fig. 3A); this mutation also eliminated a unique Pvu II cleavage site (Fig. 3B). Viral isolates containing this mutation could not replicate in Vero cells but grew to concentrations similar to those of the wild-type virus in G33 cells that stably express the UL6 protein. One isolate (KOS/UL6^m) was selected for further study. The genome of KOS/UL6^m displayed the predicted mutant Pvu II restriction pattern as determined by Southern (DNA) blot analysis (Fig. 3B).

We then tested extracts of cells infected with KOS or KOS/UL6^m for their ability to activate the two keratogenic T cell clones (*15*). Clones C1-6 and C1-15 were activated by protein extracts from Vero cells infected with wild-type HSV-1 (KOS) but not by extracts of cells infected with KOS/UL6^m (Fig. 4A), despite the fact that both extracts contained the same concentration of HSV-1 protein (Fig. 4B). Nude mice that received T cells (5×10^6) from C.AL-20 mice immunized with HSV-1–infected Vero cell extracts developed HSK, whereas recipients of the same number of T cells from mice immunized with KOS/UL6^m-infected Vero cell extracts containing the same concentration of HSV-1 protein (Fig. 4B) did not develop the disease (Fig. 4C).

To further investigate whether the HSV-1 UL6 protein contains a viral epitope that activates keratogenic T cells, we compared HSK induction by KOS/UL6^m with induction by two other replication-defective HSV-1 (KOS) mutant viruses. The HSV-1 (KOS) 5dl1.2 mutant is altered in the UL54 gene of HSV-1 encoding ICP27 and is deficient in expression of late viral proteins including UL6 (*16*). The HSV-1 mutant K082 expresses all viral proteins except the late viral protein glycoprotein B (*17*). The extent of HSK induced after corneal infection by these mutant HSV-1 strains is moderate because nonreplicating antigens placed in the eye have poor access to the immune system (*18*). Moreover, because systemic immunization of mice with HSV-1 does not increase the efficacy of disease induction because it results in production of neutralizing antibodies to HSV-1 that prevent HSK (*13*), we reconstituted CB-17 mice with severe combined immunodeficiency disease (SCID mice), which lack T and B cells and may be more sensitive to HSK induction by T cells than *nu/nu* recipients (*19*), with T cells from HSV-1–immunized C.AL-20 mice immediately before corneal infection with the different mutant HSV-1 strains. Corneal infection by the K082 mutant caused severe HSK in about 85% of these mice, whereas corneal infection with either KOS/UL6^m or KOS/5dl1.2 did not result in detectable HSK (Fig. 4D).

These data indicate that deletion of the HSV-1 (KOS) protein UL6, which stimulates self-reactive T cell clones that initiate HSK, eliminates the ability of this virus to

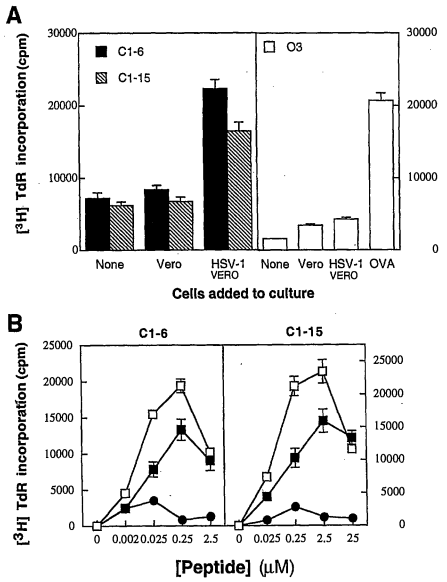

Fig. 1. (**A**) Recognition of UV-irradiated extracts of HSV-1(KOS)–infected cells by cornea-specific CD4+ T cell clones. Cornea-reactive T cell clones (C1-6 and C1-15) or the OVA-specific clone O3 (2×10^4 cells per well) were stimulated with UV-irradiated extracts of HSV-1–infected (*21*) or uninfected Vero cells in the presence of γ-irradiated [33 grays (Gy)] syngeneic BALB/c spleen cells (5×10^5 cells per well). Proliferation was assessed after 2 days by 16 to 18 hours of exposure to 1 μCi of [^{3}H]thymidine ([^{3}H]TdR) and is expressed as mean counts per minute (cpm) ± SEM of triplicate cultures. (**B**) Dose-dependent stimulation of cornea-specific CD4$^+$ T cell clones by HSV UL6-(299–314) peptide. CD4$^+$ T cell clones (C1-6 and C1-15) (2×10^4 cells per well) were incubated with the indicated peptides (0.2 μM) in the presence of irradiated (33 Gy) syngeneic BALB/c spleen cells (5×10^5 cells per well): □, p292-308 (IgG2a^b); ■, p299-314 (UL6); ●, p200-222 (MMTV). Proliferation was assessed as in (A).

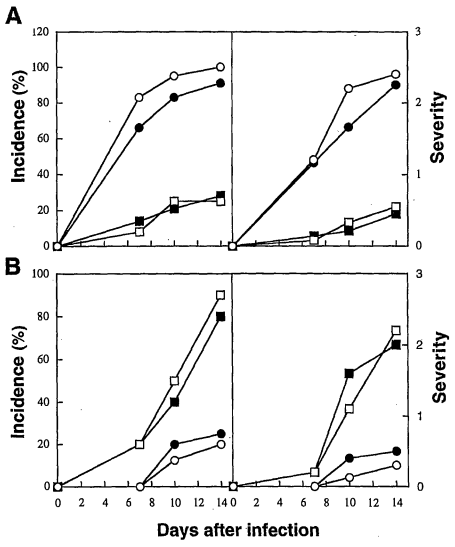

Fig. 2. Effects of HSV-1 UL6-(299–314) peptide on development of HSK. (**A**) C.AL-20 mice were injected intravenously with the indicated synthetic peptides (50 μg per mouse) in PBS 14 and 7 days before corneal infection with HSV-1 (KOS) (5×10^4 PFU per cornea): ■, p299-314 (UL6); □, p292-308 (IgG2a^b); ●, p200-222 (MMTV); ○, PBS. Disease was scored on days 7, 10, and 14 after infection as described (*9*); data are means from eight mice per group. The severity of clinical stromal keratitis in anesthetized mice was scored as described (*22*) based on the degree of corneal opacity and neovascularization: <25% of cornea, 1+; <50%, 2+; <75%, 3+; 75 to 100%, 4+. (**B**) C.AL-20 mice were immunized by injection at the base of the tail with the same peptides (50 μg per mouse) as in (A) but in complete Freund's adjuvant; ○, adjuvant alone. Two weeks later, T cells purified from pooled draining lymph nodes and spleens of immunized mice after passage through Cell-ect columns (Biotex, Edmonton, Alberta, Canada) were injected intraperitoneally into BALB/c *nu/nu* recipients (5×10^6 cells per mouse). Immediately after adoptive transfer, corneas were infected with HSV-1 (KOS) (5×10^4 PFU). Disease was scored on days 7, 10, and 14 after infection for six to eight mice per group. Additional experiments indicated that as many as 15×10^6 T cells specific for control (MMTV) peptides did not induce significant HSK.

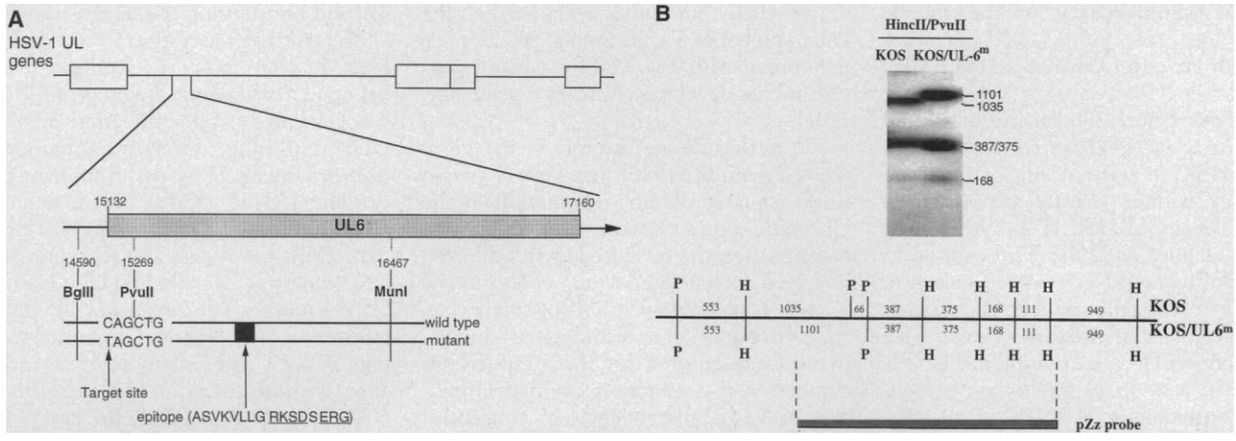

Fig. 3. (**A**) Location of the UL6 gene in the HSV-1 genome. The relative positions of UL6 restriction sites, the target mutation site, and the HSK epitope are also indicated. Amino acids are abbreviated as follows: A, Ala; S, Ser; V, Val; K, Lys; L, Leu; G, Gly; R, Arg; D, Asp; E, Glu. (**B**) Analysis of the genomic structure of the KOS/UL6^m mutant virus. DNA from KOS/UL6^m and wild-type KOS viruses was digested with Pvu II and Hinc II, and genomic fragments were separated by gel electrophoresis, transferred to nylon membranes, and subjected to Southern blot hybridization with the indicated probe (pZz). Below the blot is a restriction map for the enzymes (P, Pvu II; H, Hinc II) used in the Southern blot. The sizes of the relevant restriction fragments are indicated in base pairs.

induce HSK in mice. This effect cannot be attributed to the failure of KOS/UL6^m to replicate in corneal cells because the same concentrations of a second replication-deficient mutant, K082, that lacks a different viral structural protein (glycoprotein B) induced severe HSK. Both UL6 and glycoprotein B are late-appearing viral proteins and deletion mutants at these two loci allow expression of similar sets of HSV-1 genes (*16*, *17*). Moreover, the failure of KOS/UL6^m protein, but not of wild-type HSV-1 protein, to induce expansion of keratogenic T cells after immunization with adjuvant cannot be attributed to a replication defect. Instead, these data implicate a UL6-derived peptide in the pathogenesis of HSK.

Although viral infection can trigger autoimmune T cell responses in mice that express transgenic viral determinants (*5*, *7*), viral mimicry has not been implicated in the etiology of an autoimmune disorder that occurs after viral infection of nontransgenic animals. We have defined a viral peptide that stimulates keratogenic T cell clones in vitro and specifically modifies HSK in vivo. The finding that a mutant HSV-1 virus that lacks this epitope does not induce HSK provides direct evidence that molecular mimicry plays an important role in the development of this virally induced autoimmune disease. The identity of the corneal protein or proteins that correspond to the HSK autoantigen is not apparent from homology searches of protein databases, possibly reflecting the scarcity of structural information on murine corneal proteins in contrast to the abundance of sequence data for viruses (*6*).

The results of this study together with earlier studies suggest that susceptibility to autoimmunity after viral infection may be determined by two opposing mimicry mechanisms. Genetic polymorphisms that affect the sequence (*9*) or tissue expression (*20*) of a protein can generate endogenous molecular mimics that tolerize T cells to sequestered autoantigens and decrease susceptibility to virally induced autoimmune disease. Infection by viruses that carry an exogenous molecular mimic, as shown here, can enhance the development of autoimmunity, presumably by attraction and activation of autoreactive T cell clones to the target tissue.

We do not know whether molecular

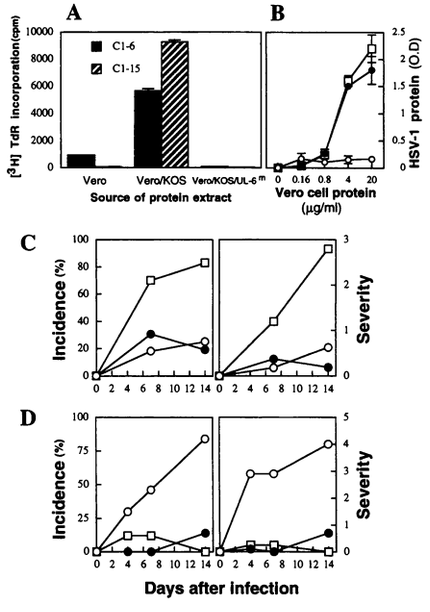

Fig. 4. Analyses of mutant strains of HSV-1 (KOS). (**A**) Keratogenic T cell clones (C1-6 and C1-15) (2 × 10^4 cells per well) were incubated with Vero cells (200 μg/ml) containing similar amounts of HSV-1 protein after infection with HSV-1 (KOS) or the mutant virus KOS/UL6^m (*21*) in the presence of irradiated (33 Gy) syngeneic BALB/c spleen cells (5 × 10^5 cells per well). Proliferation was assessed after 2 days by exposure for 16 to 18 hours to 1 μCi of [^{3}H]thymidine ([^{3}H]TdR). Results are expressed as means ± SEM of triplicate cultures. (**B**) Concentration of HSV-1 protein in Vero cell extracts 18 hours after infection with HSV-1 (KOS) (●), KOS/UL6^m (□), or after mock infection (○).HSV-1 protein was measured by a sandwich enzyme-linked immunosorbent assay in which the capture antibody was a rabbit antibody to HSV-1 (D0114, DAKO) and the secondary antibody was a peroxidase-conjugated antibody to HSV-1 (P0175, DAKO). (**C**) C.AL-20 mice were immunized (350 μg per mouse) by injection at the base of the tail with extracts of Vero cells infected with KOS/UL6^m (●) or KOS (□) or with mock-infected cells (○) emulsified in complete Freund's adjuvant. Two weeks later, purified T cells obtained from draining lymph nodes and spleens were adoptively transferred into BALB/c *nu/nu* recipients (5 × 10^6 cells per mouse). Immediately after adoptive transfer, each cornea was infected with HSV-1 (KOS) (5 × 10^4 PFU) and disease was scored on days 7, 10, and 14 after infection; data are means from 10 mice per group. (**D**) C.AL-20 mice were immunized with UV-irradiated HSV-1 (5 × 10^4 PFU per mouse). Two weeks later, T cells from immunized mice were adoptively transferred into CB-17 SCID recipients (5 × 10^6 cells per mouse). The recipients were immediately subjected to repeated corneal infection with high doses of K082 (○), KOS/UL6^m (●), or 5dl1.2 (□) mutant viruses (5 × 10^6 PFU per mouse; days 0, 2, and 4) and disease was scored 7, 10, and 14 days after the last infection. Data are means from eight mice per group.

mimicry by HSV-1 (KOS) is essential for disease induction in genetically susceptible hosts under all circumstances. Mimicry mechanisms may be particularly important in translating relatively low level viral infections into an autoimmune response. Infections by higher concentrations of HSV-1 (KOS) or by more virulent strains of HSV-1 may induce inflammatory responses that are sufficient to provoke autoimmune disease without the need for molecular mimicry. A comparison of HSK in transgenic mice with T cells that carry a receptor specific for an HSV-1 (KOS) viral peptide mimic or an unrelated peptide should further clarify the relative roles of mimicry and inflammation in the pathogenesis of virally induced autoimmune disease.

REFERENCES AND NOTES

1. W. M. Ridgway, H. L. Weiner, C. G. Fathman, *Curr. Opin. Immunol.* **6**, 946 (1994).
2. G. Dahlquist *et al.*, *Diabetologia* **38**, 1371 (1995); P. B. Challoner *et al.*, *Proc. Natl. Acad. Sci. U.S.A.* **92**, 7440 (1995); S. Vento *et al.*, *Lancet* **346**, 608 (1995).
3. E. E. Sercarz *et al.*, *Annu. Rev. Immunol.* **11**, 729 (1993).
4. B. T. Rouse, *Adv. Virus Res.* **47**, 353 (1996).
5. M. B. A. Oldstone, *Cell* **50**, 819 (1987); M. G. von Herrath and M. B. A. Oldstone, *Curr. Opin. Immunol.* **8**, 878 (1996).
6. K. W. Wucherpfennig and J. L. Strominger, *Cell* **80**, 695 (1995); B. Hemmer *et al.*, *J. Exp. Med.* **185**, 1651 (1997).
7. M. B. A. Oldstone, M. Nerenberg, P. Southern, J. Price, H. Lewicki, *Cell* **65**, 319 (1991); P. Ohashi *et al.*, *ibid.*, p. 305.
8. J. W. Streilein, M. R. Dana, B. R. Ksander, *Immunol. Today* **18**, 443 (1997).
9. A. C. Avery *et al.*, *Nature* **376**, 431 (1995).
10. M. G. Niemialtowski and B. T. Rouse, *J. Immunol.* **148**, 1864 (1992).
11. S. Friedman, D. Sillcocks, H. Cantor, *Immunogenetics* **26**, 193 (1987).
12. D. J. McGeoch *et al.*, *J. Gen. Virol.* **69**, 1531 (1997); J. Hay and W. T. Ruyechan, *Curr. Topics Microbiol. Immunol.* **179**, 1 (1992); A. H. Patel and J. B. Maclean, *Virology* **206**, 465 (1995).
13. M. B. Raizman and C. S. Foster, *Curr. Eye Res.* **7**, 823 (1988); C. S. Foster *et al.*, *Ocular Immunol. Today* (1990), p. 111.
14. The KOS/UL6^m HSV-1 mutant was constructed by using a plasmid (pSG10) containing the UL6 gene within a 10.6-kb Eco RI–generated DNA fragment derived from the genome of HSV-1 strain KOS [A. L. Goldin *et al.*, *J. Virol.* **38**, 50 (1981)]. A 1.9-kb Bgl II–Mfe I fragment from pSG10 containing a 1.3-kb segment encoding the UL6 NH_2-terminal region was subcloned into the Bam HI–Eco RI sites of pBluescript(KS) (Stratagene) to produce the plasmid pZz. A single point mutation at position 15266 (C → T) of the UL6 gene was introduced with a site-directed mutagenesis kit (Clontech) and the mutant oligonucleotide 5′-GATTCTCCTACGGG**T**AGCTGGGG-TATAC-3′ to generate a stop codon. This substitution was selected because it also eliminates the cleavage site for Pvu II (CAGCTG). The presence of the mutation in the pZz plasmid was confirmed by DNA sequencing with a Sequenase kit (U.S. Biochemical). For isolation of mutant virus, Vero cell monolayers (6 × 10^5 cells per 60-mm dish) were incubated for 24 hours after seeding and then transfected with 12 μg of DNA (including 0.5 μg of infectious KOS DNA, 5 μg of mutant plasmid DNA, and 6.5 μg of carrier DNA). Five days later, when generalized cytopathic effects were apparent, cultures were harvested and then frozen and thawed three times. The cell suspension was sonicated briefly, diluted 1:10 in medium, passed through a 0.22-μm filter, plated on monolayers of G33 cells—BHK21 cells expressing the UL6 protein [A. H. Patel *et al.*, *Virology* **217**, 111 (1996)]—and overlaid with methylcellulose. After incubation at 37°C for 4 days, plates were stained for 24 hours with medium containing neutral red, individual plaques were picked, and isolates were screened for their ability to produce cytopathic effects in G33 cells but not in Vero cells. Isolates with this phenotype were plaque-purified three times.
15. Culture flasks (75 cm^2) were seeded at a density of 1 × 10^6 Vero cells per flask. Cells were infected with wild-type KOS or KOS/UL6^m mutant viruses at a multiplicity of infection of 10 PFU per cell. Uninfected and infected cells were harvested 18 to 20 hours after infection by scraping into the medium and were centrifuged at 1500 revolutions per minute and 4°C for 10 min. The cell pellet was resuspended in 5 ml of phosphate-buffered saline (PBS), repelleted, and resuspended again in 1 ml of PBS. The cell suspension was stored at −70°C overnight, thawed at 37°C, and sonicated for 1 min. Samples were pelleted at 4°C for 10 min, and the supernatant fluid was divided into aliquots and stored at −70°C. Protein concentrations were determined by measuring absorbance at 280 nm and using bovine serum albumin as a standard.
16. A. M. McCarthy, L. McMahon, P. A. Schaffer, *J. Virol.* **63**, 18 (1989).
17. W. Cai, S. Person, S. C. Warner, J. Zhou, N. A. DeLuca, *ibid.* **61**, 714 (1987).
18. J. W. Streilein, G. A. Wilbanks, S. W. Cousins, *J. Neuroimmunol.* **39**, 185 (1992).
19. Y. A. Akova, J. Dutt, A. Rodriguez, N. Jabbur, C. S. Foster, *Curr. Eye Res.* **12**, 1093 (1993); C. M. Mercadal, D. M. Bouley, D. DeStephano, B. T. Rouse, *J. Virol.* **67**, 3404 (1993).
20. M. von Herrath, J. Dockter, M. B. A. Oldstone, *Immunity* **1**, 231 (1994).
21. The antigen used for in vitro stimulation was prepared from extracts of Vero cells infected with HSV-1 (KOS) (0.01 PFU per cell) and harvested 3 days after infection [W. Cai and P. A. Schaffer, *J. Virol.* **66**, 2904 (1992)]. The virus suspension was inactivated by UV light (254 nm) for 20 min at a distance of 5 cm [L. Morrison and D. Knipe, *J. Virol.* **68**, 689 (1994)]. Control antigen was prepared in the same way from extracts of uninfected cells.
22. E. M. Opremcak *et al.*, *Invest. Ophthalmol. Vis. Sci.* **29**, 749 (1988).

23. We would like to thank D. Knipe for providing pSG10, A. H. Patel for G33 cells, J. Glorioso for KO82 mutant virus, and A. Angel for assistance in preparation of the manuscript. Supported by NIH grant AI 37562 to H.C.

22 October 1997; accepted 7 January 1998

An Area Specialized for Spatial Working Memory in Human Frontal Cortex

Susan M. Courtney,* Laurent Petit, José Ma. Maisog, Leslie G. Ungerleider, James V. Haxby

Working memory is the process of maintaining an active representation of information so that it is available for use. In monkeys, a prefrontal cortical region important for spatial working memory lies in and around the principal sulcus, but in humans the location, and even the existence, of a region for spatial working memory is in dispute. By using functional magnetic resonance imaging in humans, an area in the superior frontal sulcus was identified that is specialized for spatial working memory. This area is located more superiorly and posteriorly in the human than in the monkey brain, which may explain why it was not recognized previously.

Studies of working memory in monkeys (*1*) and humans (*2–7*) have emphasized the important role of the prefrontal cortex. Physiological evidence for this role comes from studies demonstrating sustained activity in prefrontal cortex during working memory delays (*1*, *6–8*). In monkeys, the dorsolateral prefrontal cortex within and surrounding the principal sulcus appears to be involved primarily in working memory for spatial locations, whereas the region ventral to it on the inferior convexity appears to be more involved in working memory for patterns, colors, objects, and faces (*1*, *9*). The prefrontal region for spatial working memory in monkeys is located just anterior to a region for the control of eye movements, the frontal eye field (FEF), which is on the anterior bank of the arcuate sulcus (*10*).

Most functional brain imaging studies of spatial working memory in humans have focused on the dorsolateral frontal region defined by Brodmann as area 46 (*5*, *11*, *12*), because the spatial working memory region in monkeys lies within that area (*13*). While performance of spatial working memory tasks activates Brodmann area (BA) 46 (*5*, *11*, *12*), performance of working memory tasks involving other types of information, such as verbal and visual object information, does so as well [for example, see (*3*, *6*, *7*, *12*, *14*, *15*)]. Therefore, the existence of a prefrontal cortical area in humans that is specialized for spatial working memory has been questioned [for example, see (*16*)].

Here we provide evidence that a human frontal area specialized for spatial working

Laboratory of Brain and Cognition, National Institute of Mental Health, Building 10, Room 4C104, 10 Center Drive, Bethesda, MD 20892–1366, USA.

*To whom correspondence should be addressed. E-mail: Susan_Courtney@nih.gov